The EMBO Journal Vol. 22 No. 16 pp. 4103–4110, 2003

A signalling role for 4-hydroxy-2-nonenal in regulation of mitochondrial uncoupling

Karim S.Echtay[1], Telma C.Esteves[1], Julian L.Pakay[1], Mika B.Jekabsons[1,2], Adrian J.Lambert[1], Manuel Portero-Otín[3], Reinald Pamplona[3], Antonio J.Vidal-Puig[4], Steven Wang[5], Stephen J.Roebuck[1] and Martin D.Brand[1,6]

[1]MRC Dunn Human Nutrition Unit, Hills Road, Cambridge CB2 2XY, UK, [3]Department of Basic Medical Sciences, Faculty of Medicine, Lleida University, Lleida 25198, Spain, [4]Departments of Clinical Biochemistry and Medicine and Cambridge Institute for Medical Research, University of Cambridge, Cambridge and [5]Clore Laboratory, University of Buckingham, Buckingham MK18 1EG, UK

[2]Present address: Buck Institute, 8001 Redwood Boulevard, Novato, CA 94945, USA

[6]Corresponding author
e-mail: martin.brand@mrc-dunn.cam.ac.uk

Oxidative stress and mitochondrial dysfunction are associated with disease and aging. Oxidative stress results from overproduction of reactive oxygen species (ROS), often leading to peroxidation of membrane phospholipids and production of reactive aldehydes, particularly 4-hydroxy-2-nonenal. Mild uncoupling of oxidative phosphorylation protects by decreasing mitochondrial ROS production. We find that hydroxynonenal and structurally related compounds (such as *trans*-retinoic acid, *trans*-retinal and other 2-alkenals) specifically induce uncoupling of mitochondria through the uncoupling proteins UCP1, UCP2 and UCP3 and the adenine nucleotide translocase (ANT). Hydroxynonenal-induced uncoupling was inhibited by potent inhibitors of ANT (carboxyatractylate and bongkrekate) and UCP (GDP). The GDP-sensitive proton conductance induced by hydroxynonenal correlated with tissue expression of UCPs, appeared in yeast mitochondria expressing UCP1 and was absent in skeletal muscle mitochondria from UCP3 knockout mice. The carboxyatractylate-sensitive hydroxynonenal stimulation correlated with ANT content in mitochondria from *Drosophila melanogaster* expressing different amounts of ANT. Our findings indicate that hydroxynonenal is not merely toxic, but may be a biological signal to induce uncoupling through UCPs and ANT and thus decrease mitochondrial ROS production.

Keywords: ANT/hydroxynonenal/obesity/oxidative stress/UCP

Introduction

Mitochondria are the main intracellular producers of reactive oxygen species (ROS) in most cells and are also important targets for their harmful effects (Halliwell and Gutteridge, 1999). Mitochondrial oxidative damage may be a major factor in many human pathologies, including neurodegenerative diseases, ischaemia/reperfusion injury and inflammatory disorders (Esterbauer *et al*., 1991). Although there are several manifestations of oxidative damage to biological molecules, lipid peroxidation may be especially harmful (Esterbauer *et al*., 1991; Halliwell and Gutteridge, 1999). The polyunsaturated fatty acyl groups of membrane phospholipids are highly susceptible to peroxidation by oxygen radicals, and a self-propagating chain of free radical reactions produces various aldehydes, alkenals and hydroxyalkenals, such as malondialdehyde and 4-hydroxy-2-nonenal (HNE). Many of these products are cytotoxic, probably because of their reactivity toward proteins. Hydroxynonenal is thought to be one of the most reactive and an important mediator of free-radical damage (Esterbauer *et al*., 1991).

Hydroxynonenal can chemically modify several amino acid residues of proteins: the sulphydryl group of cysteine, the imidazole moiety of histidine and the ε-amino group of lysine (Esterbauer *et al*., 1991; Uchida and Stadtman 1992; Nadkarni and Sayre 1995; Cohn *et al*., 1996). It has broad biological toxicity: inhibition of DNA and protein synthesis, inactivation of enzymes, modification of low density lipoprotein and modulation of gene expression (Esterbauer *et al*., 1991). Mitochondrial proteins are targets of hydroxynonenal adduct formation following oxidative stress *in vivo* and *in vitro*, and hydroxynonenal inactivates the 2-oxoglutarate dehydrogenase and pyruvate dehydrogenase complexes, cytochrome *c* oxidase and NADH-linked respiration in isolated mitochondria (Humphries and Szweda, 1998; Humphries *et al*., 1998; Musatov *et al*., 2002). Here we show a novel homeostatic role of hydroxynonenal: it induces mitochondrial uncoupling by specific and inhibitable interactions with the uncoupling proteins UCP1, UCP2 and UCP3, and with the adenine nucleotide translocase (ANT). These proteins are members of a large family of at least 35 anion carriers present in the mitochondrial inner membrane (Bouillaud *et al*., 2001). Mild uncoupling decreases mitochondrial production of ROS, which can subsequently cause hydroxynonenal production (Papa and Skulachev, 1997). This suggests a negative feedback loop in which hydroxynonenal signals damage by ROS and decreases ROS production through induction of uncoupling by UCPs and ANT.

Results and discussion

Figure 1 shows that HNE increased the proton conductance of isolated rat kidney mitochondria. Respiration driving the leak of protons across the membrane at any particular membrane potential was faster in the presence of hydroxynonenal than in its absence, resulting in a kinetic curve that was displaced upwards (see Cadenas *et al*.,

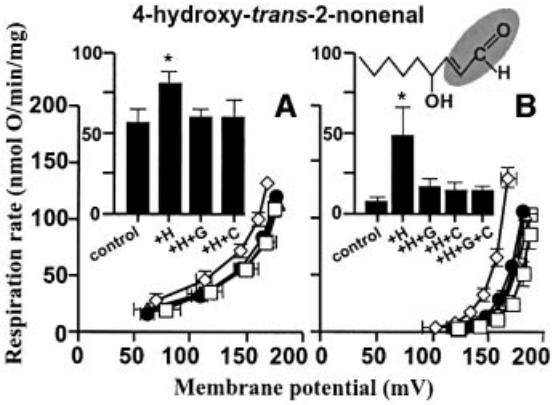

Fig. 1. Hydroxynonenal activation of proton conductance through UCP2 and ANT: effect of HNE on proton leak kinetics in rat kidney mitochondria. Proton leak kinetics were measured as described in Materials and methods: (**A**) without BSA in the presence of 1 μM HNE; (**B**) in the presence of BSA and 35 μM HNE. Squares, control; diamonds, HNE (+H); filled circles, HNE plus 500 μM GDP (+H+G); triangles, HNE plus 2.5 μM CAT (+H+C); crossed squares, HNE plus GDP and CAT (+H+G+C). Inserts show respiration rates driving proton leak at 150 mV for the same dataset. Data are means ± SEM of three independent experiments each performed in duplicate. **P* <0.05 versus control.

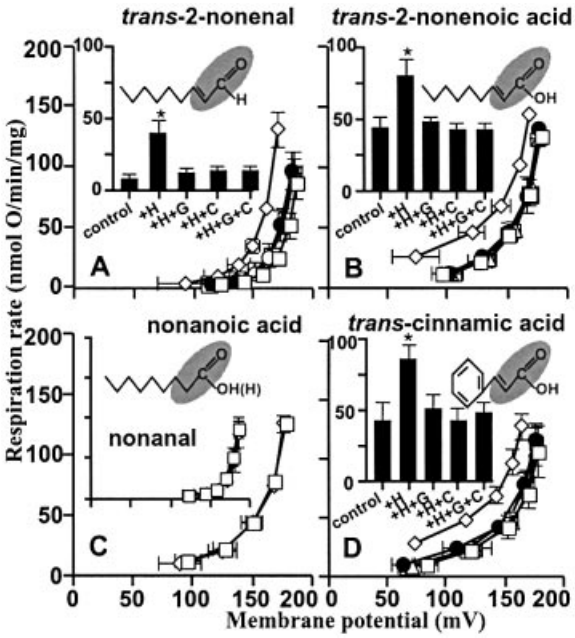

Fig. 2. Hydroxynonenal activation of proton conductance through UCP2 and ANT: effects of compounds related to HNE on proton leak kinetics in rat kidney mitochondria. Proton leak kinetics were measured as described in Materials and methods in the presence of: (**A**) BSA and 35 μM *trans*-2-nonenal; (**B**) 35 μM *trans*-2-nonenoic acid; (**C**) 35 μM nonanoic acid (insert: BSA and 35 μM nonanal); (**D**) 50 μM cinnamic acid. Squares, control; diamonds, studied compound (+H); filled circles, compound plus 500 μM GDP (+H+G); triangles, compound plus 2.5 μM CAT (+H+C); crossed squares, compound plus GDP and CAT (+H+G+C). Inserts in (A), (B) and (D) show respiration rates driving proton leak at 150 mV for the same dataset. Data are means ± SEM of three independent experiments each performed in duplicate. **P* <0.05 versus control.

2002; Echtay *et al*., 2002a,b). A strong effect was seen with 35 μM hydroxynonenal (Figure 1B), but the increase in proton conductance was also detected at 1 μM

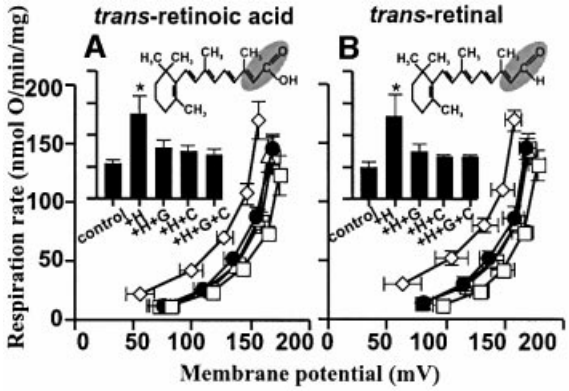

Fig. 3. Hydroxynonenal activation of proton conductance through UCP2 and ANT: effects of retinoic acid and retinal on proton leak kinetics in rat kidney mitochondria. Proton leak kinetics were measured as described in Materials and methods in the presence of: (**A**) 5 μM *trans*-retinoic acid; (**B**) 5 μM *trans*-retinal. Squares, control; diamonds, studied compound (+H); filled circles, compound plus 500 μM GDP (+H+G); triangles, compound plus 2.5 μM CAT (+H+C); crossed squares, compound plus GDP and CAT (+H+G+C). Inserts show respiration rates driving proton leak at 150 mV for the same dataset. Data are means ± SEM of three independent experiments each performed in duplicate. **P* <0.05 versus control.

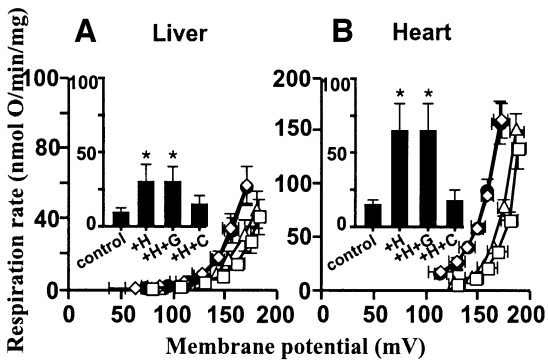

Fig. 4. Effect of hydroxynonenal on mitochondrial proton conductance through ANT. Proton leak kinetics in mitochondria from (**A**) liver and (**B**) heart were measured as described in Materials and methods in the presence of BSA. Squares, control; diamonds, plus 35 μM HNE (+H); filled circles, HNE plus 500 μM GDP (+H+G); triangles, HNE plus 2.5 μM CAT (+H+C). Inserts show respiration rates driving proton leak at 150 mV for the same dataset. Data are means ± SEM of three independent experiments each performed in duplicate. **P* <0.05 versus control.

hydroxynonenal (Figure 1A). This was not simply due to non-specific damage to the membrane, since it was fully prevented by GDP or by carboxyatractylate (CAT) (Figure 1). Results discussed below show that this increase in proton conductance was mediated through UCP2 and ANT. Unlike superoxide-induced uncoupling (Echtay *et al*., 2002a), hydroxynonenal-induced uncoupling occurred in the presence of defatted bovine serum albumin (BSA), and did not require added fatty acids.

The structural requirements of hydroxynonenal for activation of proton conductance are explored in Figure 2. *Trans*-2-nonenal (Figure 2A) had the same effects as HNE, showing that the 4-hydroxyl was not required. *Trans*-2-nonenoic acid (Figure 2B) was also effective, showing that the aldehyde could be replaced by

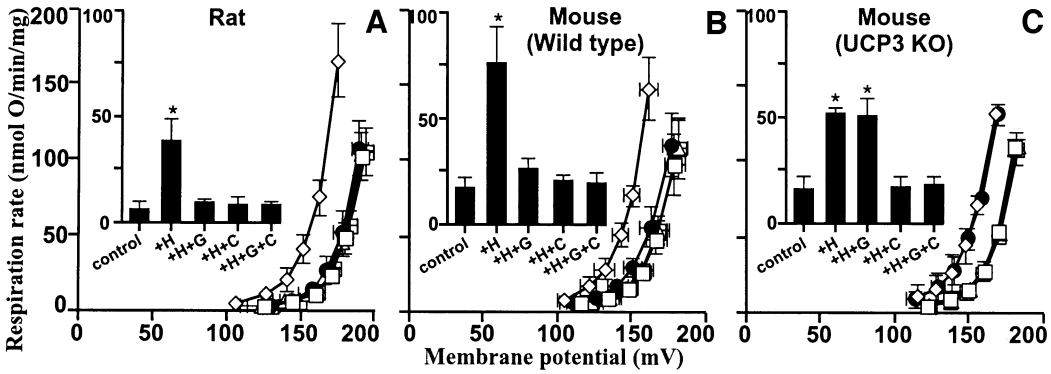

Fig. 5. Hydroxynonenal activation of proton conductance through UCP3 and ANT. Proton leak kinetics were measured as described in Materials and methods in the presence of BSA in mitochondria from: (**A**) rat skeletal muscle; (**B**) skeletal muscle from wild-type mice; (**C**) skeletal muscle from *ucp3–/–* mice (Echtay *et al*., 2002a). Squares, control; diamonds, 35 μM HNE (+H); filled circles, HNE plus 500 μM GDP (+H+G); triangles, HNE plus 2.5 μM CAT (+H+C). Inserts show respiration rates driving proton leak at 150 mV for the same dataset. Data are means ± SEM of three independent experiments each performed in duplicate. **P* <0.05 versus control.

carboxyl. However, there was no effect of the saturated analogues nonanal and nonanoic acid (Figure 2C), which lack the double bond at carbon-2, indicating that this double bond is required. We suggest that the reactive 2-alkenal functional group modifies specific residues in the UCPs and ANT, leading to increased proton transport activity. Interestingly, cinnamic acid (Figure 2D), *trans*-retinoic acid (Figure 3A) and *trans*-retinal (Figure 3B), which all contain this functional group, also induced GDP- and carboxyatractylate-sensitive proton conductance.

Is UCP2 involved in the activation of proton conductance by hydroxynonenal in kidney mitochondria? The mRNA for UCP2 is found in kidney (Zhang *et al*., 2001; Couplan *et al*., 2002) but the mRNA for UCP3 is not (Boss *et al*., 1997), while UCP1 is found only in brown adipose tissue (BAT), so UCP2 is the only candidate UCP in kidney mitochondria. Western blot evidence for the presence of UCP2 protein in rodent kidney mitochondria is ambiguous, because of poor antibody specificity (Pecqueur *et al*., 2001). Couplan *et al*. (2002) failed to detect UCP2 in kidney mitochondria, but careful examination of their western blots suggests that UCP2 is expressed there at low levels, since the intensity of the immunoreactive band at ~30 kDa was diminished in kidney mitochondria from *ucp2–/–* mice. Evidence for UCP2 in kidney mitochondria is stronger using functional tests. Purine nucleotides bind to UCP2 (Echtay *et al*., 2001; Jekabsons *et al*., 2002). They also inhibit superoxide-inducible proton conductance through UCP1 in BAT mitochondria and UCP3 in skeletal muscle mitochondria (Echtay *et al*., 2002a), and sensitivity to GDP appears to be diagnostic of UCP involvement in mitochondrial proton conductance. GDP inhibits superoxide-inducible proton conductance in kidney mitochondria (Echtay *et al*., 2002a), strongly suggesting that UCP2 is present in these mitochondria.

Hydroxynonenal-inducible proton conductance in kidney mitochondria was sensitive to GDP (Figure 1), suggesting that activation by hydroxynonenal is mediated by UCP2. Figure 4A and B shows that although hydroxynonenal stimulated proton conductance in mitochondria from liver and heart, tissues that lack UCPs (Pecqueur *et al*., 2001; Echtay *et al*., 2002a), GDP was not inhibitory, consistent with the absence of UCP2 in these tissues.

To explore whether UCP3 could also respond to hydroxynonenal, we examined the effect of hydroxynonenal on skeletal muscle mitochondria, which contain UCP3 but not UCP1 or UCP2 (Bouillaud *et al*., 2001; Pecqueur *et al*., 2001; Echtay *et al*., 2002a). Figure 5A shows that hydroxynonenal induced proton conductance in the absence, but not in the presence, of GDP. Confirmation of the role of UCP3 was obtained using skeletal muscle mitochondria from *ucp3* knockout mice (Cadenas *et al*., 2002; Echtay *et al*., 2002a). Hydroxynonenal caused GDP-sensitive stimulation of proton conductance in skeletal muscle mitochondria from wild-type mice (Figure 5B), as it did in rats. However, hydroxynonenal stimulation of proton conductance was significantly less in *ucp3* knockout compared with wild-type mitochondria, and GDP did not prevent this hydroxynonenal stimulation (Figure 5C). These results show that hydroxynonenal can uncouple skeletal muscle mitochondria through a GDP-sensitive interaction with UCP3.

To determine whether UCP1 is also activated by hydroxynonenal, we examined mitochondria from warm-adapted rat BAT, which (unlike mitochondria from cold-adapted rats) contain sufficiently low amounts of UCP1 to permit coupling in the absence of added nucleotides (Echtay *et al*., 2002a). Figure 6 shows that GDP inhibited the endogenous UCP1 activity, lowering the control proton conductance to the basal level. Hydroxynonenal increased proton conductance substantially in the control without GDP, but stimulated it very little above basal in the presence of GDP (Figure 6), suggesting that uncoupling by UCP1 is also activated by hydroxynonenal. However, *UCP2* and *UCP3* mRNA (but not UCP2 protein) are also present in BAT (Ricquier and Bouillaud, 2000; Pecqueur *et al*., 2001), possibly weakening this conclusion. Confirmation of the role of UCP1 was obtained using yeast mitochondria expressing mouse UCP1 (Stuart *et al*., 2001; Echtay *et al*., 2002a). Mitochondria from control yeast containing empty vector showed little uncoupling by hydroxynonenal, and no effect of GDP (Figure 7A) (so yeast ANT, unlike the mammalian protein, is insensitive to HNE at the concentration used).

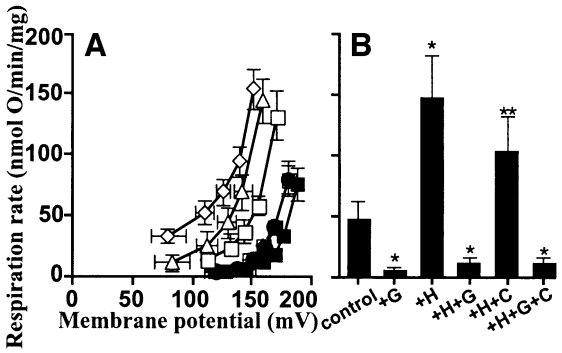

Fig. 6. Hydroxynonenal activation of proton conductance through UCP1 and ANT in BAT mitochondria. Proton leak kinetics were measured as described in Materials and methods in the presence of BSA (1%) in mitochondria from warm-adapted rat BAT. (**A**) Leak kinetics: squares, control; filled squares, control plus 500 μM GDP (+G); diamonds, 50 μM HNE (+H); filled circles, HNE plus 500 μM GDP (+H+G); triangles, HNE plus 2.5 μM CAT (+H+C); crossed squares, HNE plus GDP and CAT (+H+G+C). (**B**) Respiration rates driving proton leak at 150 mV for the same dataset. Data are means ± SEM of three independent experiments each performed in duplicate. **P* <0.05 versus control; ***P* <0.05 versus +H.

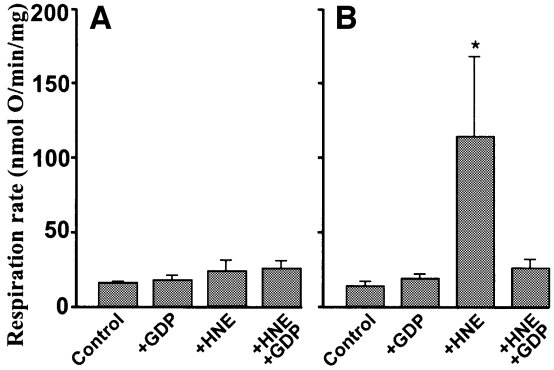

Fig. 7. Hydroxynonenal activation of proton conductance through mouse UCP1 expressed in yeast mitochondria. Proton leak kinetics were measured as described in Materials and methods in mitochondria from: (**A**) yeast containing control empty vector; (**B**) yeast expressing mouse UCP1. Respiration rates driving proton leak were interpolated from the leak kinetics at 82 mV. Data are means ± SEM of three independent experiments each performed in duplicate. * *P* <0.05 versus control.

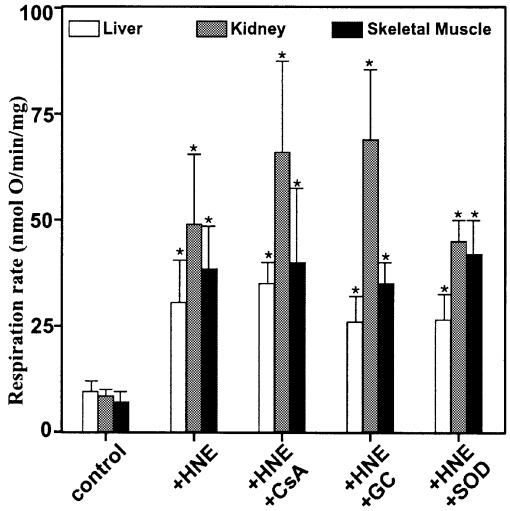

Fig. 8. Hydroxynonenal activation of proton leak. Mitochondria from rat liver, kidney, and skeletal muscle were incubated as described in Materials and methods in the presence of BSA. 35 μM HNE, 500 μM GDP, 2.5 μM CAT, 1 μM cyclosporin A (CSA), 1 μM glybenclamide (GC) and 12 U.ml^{-1} superoxide dismutase (SOD) were present where indicated. Respiration rates driving proton leak were interpolated from the leak kinetics at 150 mV. Data are means ± SEM of three independent experiments each performed in duplicate. **P* <0.05 versus control.

In contrast, hydroxynonenal markedly stimulated the proton conductance of mitochondria from yeast expressing UCP1, and this stimulation was prevented by GDP (Figure 7B). These results clearly show that hydroxynonenal increases GDP-sensitive proton conductance through UCP1. There is abundant evidence in the literature that UCP1 activation in BAT mitochondria causes stimulation of respiration by altering proton conductance, and not by causing slip of the proton pumps in the electron transport chain. The hydroxynonenal activation of respiration in UCP1-containing (but not control) yeast mitochondria and the lack of GDP-sensitive hydroxynonenal activation in UCP3 knockout mouse mitochondria show that hydroxynonenal alters the relationship between respiration rate and membrane potential by increasing proton conductance through the UCPs, and not by stimulating slip in electron transport.

Taken together, the results discussed above show that UCP1, UCP2 and UCP3 can each catalyse hydroxynonenal-induced GDP-sensitive proton conductance. However, it was also clear that a component of the hydroxynonenal effect persisted in mitochondria lacking UCPs (Figures 4A and B, and 5C). Stimulation by hydroxynonenal was not prevented by glybenclamide, a K_{ATP} channel blocker, or cyclosporin A, an inhibitor of the mitochondrial permeability transition (Figure 8). It was insensitive to superoxide dismutase, required ~2 min reaction time and was not fully reversible, since GDP (or carboxyatractylate) added after hydroxynonenal was only partially inhibitory.

The ubiquitous ANT is a fourth target for hydroxynonenal. Carboxyatractylate (CAT) (Figures 1, 4 and 5) and bongkrekate (BKA) (Figure 9), potent and highly specific inhibitors of ANT (Klingenberg, 1975), strongly inhibited uncoupling induced by hydroxynonenal in mitochondria from kidney, liver, heart and skeletal muscle. ANT is present in BAT mitochondria at about the same concentration as it is in liver mitochondria (Chavez *et al.*, 1996), and in BAT mitochondria (Figure 6) carboxyatractylate inhibited hydroxynonenal-induced uncoupling by about the same absolute extent as it did in liver mitochondria (Figure 4A). However, because of the high UCP1 concentration in BAT mitochondria, the percentage inhibition by carboxyatractylate was much less than it was in mitochondria from the other tissues. Confirmation of the role of ANT was obtained using mitochondria from *Drosophila melanogaster* expressing different amounts of ANT (M.D.Brand, unpublished observation), where hydroxynonenal stimulation correlated well with ANT content (Figure 10). This stimulation in *Drosophila* was completely sensitive to carboxyatractylate and insensitive to GDP (not shown), confirming that ANT catalyses hydroxynonenal-induced proton conductance. The effect of varying ANT was not due to non-

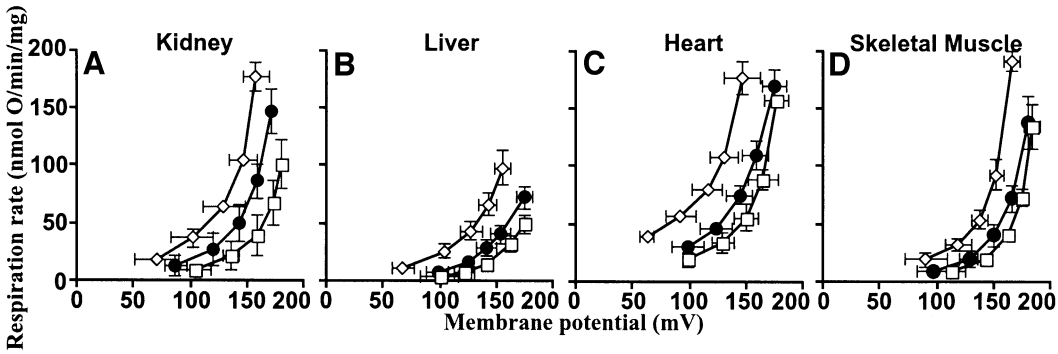

Fig. 9. Hydroxynonenal activation of proton conductance through ANT: effect of BKA. Mitochondria from different rat tissues were incubated as described in Materials and methods without BSA. (**A**) Kidney; (**B**) liver; (**C**) heart; (**D**) skeletal muscle. Squares, control; diamonds, plus 35 μM HNE; filled circles, HNE plus 8 μM BKA. Data are means ± SEM of three independent experiments each performed in duplicate.

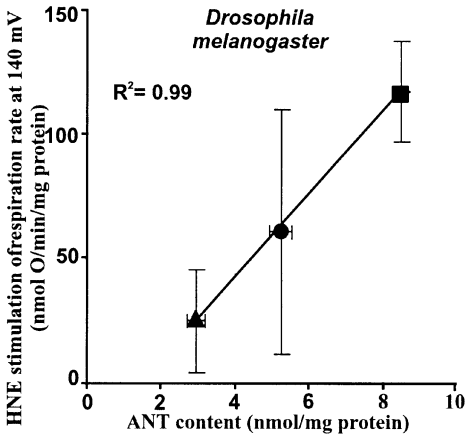

Fig. 10. Dependence of hydroxynonenal activation on ANT content in *Drosophila* mitochondria. Proton leak was measured as described in Materials and methods with 2 mM $MgCl_2$ and 0.3% (w/v) BSA present, at 25°C, using 10 mM glycerol 3-phosphate as substrate and titrating with cyanide up to ~200 μM. The stimulation of respiration by 35 μM HNE was interpolated from the leak kinetics at the highest common potential (140 mV). ANT content was measured by titration with CAT. Circle, wild-type flies; triangle, *sesB*+/– flies (*sesB* codes for ANT; Zhang *et al*., 1999); square, flies with a 10.3 kb fragment containing *sesB* inserted into chromosome 2 or 4. Data are means ± SEM of six independent experiments each performed in duplicate.

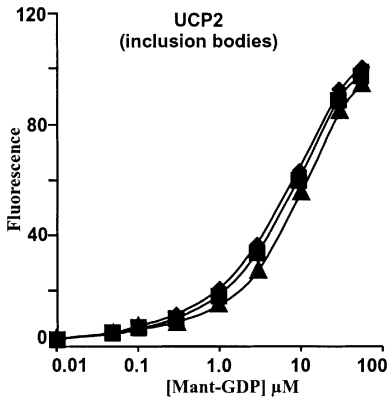

Fig. 11. Effect of CAT on nucleotide binding to UCP2. Fluorescence binding measurement of Mant-GDP to renatured UCP2 inclusion bodies was performed as described in Materials and methods. Diamonds, no CAT; squares, plus 1 μM CAT; triangles, plus 10 μM CAT.

specific damage to the membrane as a result of over-expression of a mitochondrial protein, since the extra HNE activation was still fully sensitive to CAT.

Despite the clear demonstration that hydroxynonenal can induce proton conductance through both UCPs and ANT, there were perplexing effects of GDP and carboxyatractylate: where both types of carrier were present, the inhibitors were not fully additive. Thus, in kidney (Figure 1) or skeletal muscle (Figure 5), either inhibitor alone was as effective as both together. This was not due to lack of specificity of the inhibitors, as there was no effect of carboxyatractylate on binding of fluorescently tagged GDP to UCP2 (Figure 11), and carboxyatractylate had only small percentage effects in BAT mitochondria, which have little ANT relative to UCP1 (Figure 6). Conversely, GDP had no effect in mitochondria lacking UCPs (Figures 4A and B, 5C). We speculate that hydroxynonenal traps ANT and UCP in a heterodimer that is sensitive to either inhibitor.

Retinoic acid is a powerful activator of *ucp1* gene expression, working through nuclear receptors (Alvarez *et al*., 1995). It also directly activates proton transport through UCP1 and UCP2 (Rial *et al*., 1999). Our observations confirm that retinoic acid can activate GDP-sensitive proton transport (by UCP2) in kidney mitochondria, and show that it can also induce carboxyatractylate-sensitive proton conductance through ANT (Figure 3A). The carboxylic acid group of retinoic acid is not required, as retinal (in contrast to Rial *et al*., 1999) has the same effects (Figure 3B). Retinoic acid, retinal and the more potent analogue TTNPB (Rial *et al*., 1999) all contain the same 2-alkenal functional group as hydroxynonenal, so we propose that they too induce proton transport by modifying particular residues in UCPs and ANT, rather than acting as inert ligands. They may be more promising than the more toxic hydroxynonenal as lead compounds for the development of anti-obesity pharmaceuticals that work by specifically activating mitochondrial uncoupling by UCPs (Harper *et al*., 2001).

Superoxide induces uncoupling through the UCPs (Echtay *et al*., 2002a). We investigated the hypothesis that superoxide, by initiating lipid peroxidation, releases hydroxynonenal as a second messenger that is the direct inducer of proton conductance by the UCPs (data not shown). There are differences between the two activators:

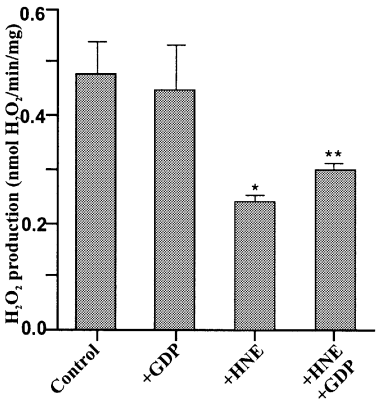

Fig. 12. Hydroxynonenal decreases mitochondrial ROS production. H_2O_2 production by kidney mitochondria was measured as described in Materials and methods in the presence of 10 μM HNE and 500 μM GDP as indicated. Data are means ± range of two independent experiments each performed in duplicate. **P* <0.05 versus control; ***P* <0.05 versus +HNE.

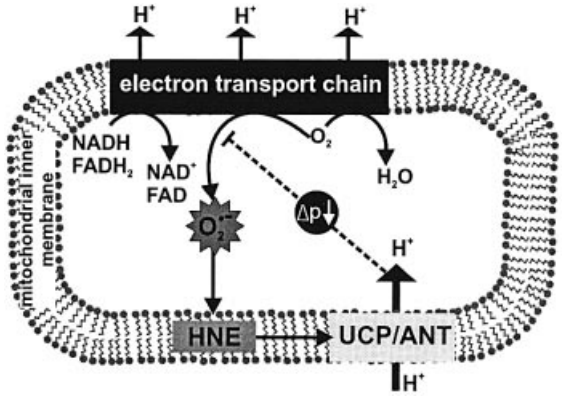

Fig. 13. Signalling role of hydroxynonenal. During oxidation of substrates, the complexes of the mitochondrial electron transport chain reduce oxygen to water, and pump protons into the intermembrane space, forming a proton motive force (Δp). However, some electrons in the reduced complexes also react with oxygen to produce superoxide. Superoxide can peroxidize membrane phospholipids, forming hydroxynonenal, which induces proton transport through UCPs and ANT. The mild uncoupling caused by proton transport lowers Δp and slightly stimulates electron transport, causing the complexes to become more oxidized and lowering the local concentration of oxygen; both these effects decrease superoxide production. Thus induction of proton leak by hydroxynonenal limits mitochondrial ROS production as a feedback response to overproduction of superoxide by the respiratory chain.

the effect of superoxide requires added fatty acids and is insensitive to carboxyatractylate and specific for the UCPs (Echtay *et al*., 2002a), whereas hydroxynonenal does not require fatty acids and also targets ANT. Treatment of kidney mitochondria with superoxide exactly as in Echtay *et al*. (2002a) did not produce detectable amounts of hydroxynonenal using a commercial assay kit (Calbiochem). There was no change in the fatty acyl composition of the phospholipids, in the double bond and peroxidizability indices, or in five markers of different kinds of oxidative damage to proteins [assayed by GC/MS as described by Portero-Otín *et al*. (1999) and Brand *et al*. (2002)]. We also found that oxidized forms of arachidonic and linoleic acids, 8(S)-HETE (8S-hydroxy-5Z,9E,11Z, 14Z-eicosatetraenoic acid) and 9-HODE [(±)9-hydroxy-10E,12Z-octadecadienoic acid] had no effect on proton conductance. Thus, we have no evidence that hydroxynonenal (or another lipid peroxidation product) mediates activation of UCPs by superoxide. However, the amounts of hydroxynonenal involved might be too low to be detected by our assays. The effects of superoxide and hydroxynonenal were found to be non-additive, supporting the hypothesis that they activate the same process.

Figure 12 shows that mitochondrial ROS production was sensitive to hydroxynonenal (see below).

Conclusion

The results presented here show that physiologically relevant concentrations of HNE, a major product of oxidant-induced peroxidation of membrane phospholipids, specifically uncouple mitochondria. Structurally related compounds, such as *trans*-2-nonenal, *trans*-2-nonenoic acid, *trans*-retinoic acid, *trans*-retinal and other molecules containing the reactive 2-alkenal group have the same effect, suggesting that the alkenal group of these compounds reacts with a target protein in the mitochondria. Hydroxynonenal-induced uncoupling was inhibited by GDP, a potent inhibitor of uncoupling proteins UCP1, UCP2 and UCP3, and by CAT and BKA, potent inhibitors of the adenine nucleotide translocase. The GDP-sensitive proton conductance induced by hydroxynonenal was absent in skeletal muscle mitochondria from UCP3 knockout mice, appeared in yeast mitochondria expressing UCP1, and correlated with tissue expression of UCPs, demonstrating that it acted through the UCPs. The carboxyatractylate-sensitive hydroxynonenal stimulation of proton conductance correlated with adenine nucleotide translocase content in mitochondria from *D.melanogaster* expressing different amounts of the *sesB* gene product. This, together with the inhibitor specificity, shows that hydroxynonenal also acts through the adenine nucleotide translocase.

Our results suggest a physiological negative feedback signalling function for hydroxynonenal. Oxidative stress (for example during aging or ischaemia/reperfusion) can alter the activity of the adenine nucleotide translocase: it leads to mitochondrial swelling and damage (Kristal *et al*., 1996; Ullrich *et al*., 1996) related to induction of the permeability transition pore activity of translocase, and it compromises nucleotide transport by this carrier (Nohl and Kramer, 1980; Chen *et al*., 1995; Yan and Sohal, 1998). Oxidative stress can also induce UCP2 expression (Pecqueur *et al*., 2001) and mice lacking UCP3 produce more ROS than wild-type mice (Vidal-Puig *et al*., 2000; Brand *et al*., 2002). Hydroxynonenal may be involved in some of these effects: oxidative stress can lead to a hydroxynonenal–protein adduct at 32 kDa (corresponding to the molecular weights of the adenine nucleotide translocase and the UCPs) (Kirichenko *et al*., 1996), and hydroxynonenal inhibits ADP transport by the adenine nucleotide translocase (Nohl and Kramer, 1980; Chen *et al*., 1995). In addition, free radical-mediated lipid peroxidation and the associated production of hydroxynonenal could affect the function of these proteins by compromising the phospholipids of the mitochondrial inner membrane (Chen and Yu, 1994). Together with the results reported here, these findings suggest that oxidative stress, via 2-alkenal products such as hydroxynonenal,

can alter the uncoupling, transport and pore functions of the adenine nucleotide translocase and the UCPs. Hydroxynonenal may be not only a toxic product of oxidative damage, but also an important signal that decreases ROS production (Figure 13). Mitochondrial ROS production would lead to lipid peroxidation and hydroxynonenal production. Hydroxynonenal would induce mild uncoupling by UCPs and the adenine nucleotide translocase, thus lowering the mitochondrial membrane potential and decreasing ROS production, which is very sensitive to membrane potential (Papa and Skulachev, 1997). Mild uncoupling would also lead to increased oxygen consumption, depleting the local concentration of oxygen and reinforcing the decrease in ROS production (Papa and Skulachev, 1997). This sequence of events would provide an effective local feedback control over harmful ROS production (Figure 13): extra ROS production would increase HNE, which would activate mild uncoupling and attenuate the rise in ROS production. In support of this possibility, muscle mitochondria from UCP3 KO mice have increased oxidative damage to aconitase (Vidal-Puig *et al*., 2000) and membrane phospholipids (Brand *et al*., 2002).

To examine this hypothesis, we investigated the effect of hydroxynonenal on ROS production by isolated kidney mitochondria. Figure 12 shows that hydroxynonenal did indeed decrease ROS production as predicted. This decrease is consistent with the decrease in membrane potential caused by hydroxynonenal (Figure 1). GDP partially protected ROS production against the effect of hydroxynonenal (Figure 12) consistent with its incomplete protection of membrane potential (Figure 1) and with the involvement of UCP2 as predicted by our model.

The hydroxynonenal concentration that activates UCPs and the adenine nucleotide translocase is within the micromolar physiological concentrations estimated *in vivo* (Esterbauer *et al*., 1991; Halliwell and Gutteridge, 1999), as predicted for a mechanism designed to come into action only during mild oxidative stress. Under more severe oxidative stress, the permeability transition pore function of the translocase (and UCPs?) would be engaged as part of the more powerful apoptotic defence against free radicals (Kristal *et al*., 1996; Papa and Skulachev, 1997).

Materials and methods

Chemical reagents

HNE, [8(S)-HETE] 8S-hydroxy-5Z,9E,11Z,14Z-eicosatetraenoic acid and (9-HODE) (±)9-hydroxy-10E,12Z-octadecadienoic acid were obtained from Cayman. *N*-methylanthraniloyl (Mant)-GDP was from Molecular Probes. Retinoic acid (*all-trans*), retinal (*all-trans*), *trans*-2-nonenoic acid and nonanoic acid were from Sigma. Nonanal and *trans*-2-nonenal were from Acros Organics.

Isolation of mitochondria

Mitochondria from liver, kidney, heart, total hindlimb skeletal muscle and BAT were prepared essentially as described previously (Cadenas *et al*., 2002; Echtay *et al*., 2002a, b), with all steps carried out at 4°C. Tissues were homogenized using a glass Dounce homogenizer in isolation medium containing 250 mM sucrose, 5 mM Tris–HCl (pH 7.4) and 2 mM EGTA. For BAT mitochondria the isolation medium was supplemented with 1% (w/v) BSA. Mitochondria were collected at 11 621 *g* and washed at 1047 *g*. Mitochondrial pellets were suspended in isolation medium and protein concentration was determined by the biuret method. All results are expressed per mg mitochondrial protein.

Yeast mitochondria were isolated as described previously (Stuart *et al*., 2001). Mitochondrial pellets were suspended in 10 mM Tris/maleate, 650 mM sorbitol and 2 mM EGTA, pH 6.8.

Drosophila mitochondria were prepared by homogenizing adult female *D.melanogaster* in ice-cold medium [250 mM sucrose, 5 mM Tris–HCl, 2 mM EGTA, 1 % (w/v) BSA, pH 7.4 at 4°C]. The homogenate was filtered through two layers of muslin and centrifuged at 150 *g* for 3 min at 4°C. The supernatant was then filtered through one layer of muslin and centrifuged at 9000 *g* for 10 min. The mitochondrial pellet was resuspended in assay medium [120 mM KCl, 5 mM KH_2PO_4, 3 mM HEPES, 1 mM EGTA, 2 mM $MgCl_2$ and 0.3% (w/v) BSA] and protein concentration was determined using the Bio-Rad DC protein assay kit with BSA as a standard.

Proton leak measurements

The kinetics of proton conductance were measured in non-phosphorylating mitochondria to avoid interference by any changes in the rate of respiration driving phosphorylation. These kinetics will then describe the behaviour of the leak pathway under many other conditions, including those where ATP is being made. Mitochondria from skeletal muscle (0.35 mg/ml), liver (0.5 mg/ml), kidney (0.35 mg/ml) or heart (0.35 mg/ml) were incubated in standard assay medium containing 120 mM KCl, 5 mM KH_2PO_4, 3 mM HEPES and 1 mM EGTA (pH 7.2, 37°C), with 5 μM rotenone, 80 ng nigericin/ml and 1 μg oligomycin/ml. Defatted BSA (0.3%) was added where indicated. Respiration rate and membrane potential were measured simultaneously using electrodes sensitive to oxygen and to triphenylmethylphosphonium ($TPMP^+$) (Cadenas *et al*., 2002; Echtay *et al*., 2002a,b). The TPMP electrode was calibrated with five sequential 0.5 μM additions of $TPMP^+$, then 4 mM succinate was added as substrate. Membrane potential was varied by adding malonate (up to 1 mM). After each run, 0.2 μM FCCP was added to release $TPMP^+$ for baseline correction. A TPMP binding correction of 0.4/(μl per mg protein) was used. This correction takes into account any changes in matrix volume that may have occurred (Brand, 1995).

Proton leak in BAT mitochondria (0.35 mg/ml) isolated from rats maintained at 25°C was measured in assay medium containing 50 mM KCl, 5 mM HEPES, 1 mM EGTA, 4 mM KH_2PO_4, pH 7.2, at 37°C, with 5 μM rotenone, 80 ng nigericin/ml and 1 μg oligomycin/ml, and supplemented with 1% (w/v) defatted BSA. Titration was by addition of cyanide (up to ~100 μM) using 10 mM glycerol 3-phosphate as substrate. The whole proton leak kinetic measurements took up to ~10 min.

Proton leak in yeast mitochondria (0.6 mg/ml) was measured in medium [20 mM Tris–HCl, 450 mM sorbitol, 100 mM KCl, 0.5 mM EGTA, 5 mM $MgCl_2$, 10 mM K_2HPO_4, and 0.1% (w/v) defatted BSA, pH 6.8, 30°C] plus 50 μM palmitate, 1 μg nigericin/ml, 0.1 μg oligomycin/ml, 3 μM myxothiazol and 8 mM ascorbate. Membrane potential was varied by titration with *N*,*N*,*N*′,*N*′-tetramethyl-*p*-phenylenediamine up to 125 μM.

Expression of UCP1 in Saccharomyces cerevisiae

UCP1 was expressed in the diploid yeast *S.cerevisiae* strain CEN.PK2-1C transformed with vector pBF307 which contains the coding sequence for mouse UCP1 as described previously (Stuart *et al*., 2001). Gene expression was under the control of the GAL1 promoter.

Bacterial expression, isolation, renaturation and nucleotide binding to inclusion bodies containing UCP2

Human UCP2 expression, purification and refolding from bacterial inclusion bodies were performed as described in Jekabsons *et al*. (2002). Nucleotide binding to UCP2 inclusion bodies was measured by fluorescence resonance energy transfer. UCP2 was diluted to 90 μg/ml in 20 mM MOPS, 0.1 mM EDTA, pH 6.8, at 10°C and titrated with Mant-GDP using λ_{ex} = 280 nm, λ_{em} = 433 nm and 1.5 nm slit width.

Measurement of mitochondrial H_2O_2 production

Hydrogen peroxide generation rates were determined fluorometrically by measurement of oxidation of *p*-hydroxyphenyl acetic acid (PHPA) coupled to the enzymatic reduction of H_2O_2 by horseradish peroxidase. Kidney mitochondria (0.35 mg/ml) were incubated in standard incubation buffer (120 mM KCl, 5 mM KH_2PO_4, 3 mM HEPES, 1 mM EGTA and 0.3% BSA, pH 7.2, 37°C), without rotenone and containing 50 μg/ml PHPA, 4 U/ml horseradish peroxidase, 30 U/ml superoxide dismutase, 1 μg/ml oligomycin and 80 ng/ml nigericin. After addition of 4 mM succinate the increase in fluorescence at an excitation of 320 nm and emission of 400 nm was followed on a computer-controlled spectrofluorimeter with appropriate correction for background and use of a standard curve as described in St-Pierre *et al*. (2002).

Acknowledgements

We thank Mike Ashburner and John Roote (Department of Genetics, University of Cambridge, UK) for supplying the *Drosophila* mutants, and Julie Buckingham, Michael Cawthorne, Emma Cornwall, Katherine Green, Satomi Miwa, Mike Murphy and Darren Talbot for assistance and discussions.

References

Alvarez,R., de Andres,J., Yubero,P., Vinas,O., Mampel,T., Iglesias,R., Giralt,M. and Villarroya,F. (1995) A novel regulatory pathway of brown fat thermogenesis. Retinoic acid is a transcriptional activator of the mitochondrial uncoupling protein gene. *J. Biol. Chem.*, **270**, 5666–5673.

Boss,O., Samec,S., Paoloni-Giacobino,A., Rossier,C., Dulloo,A., Seydoux,J., Muzzin,P. and Giacobino,J.-P. (1997) Uncoupling protein-3: a new member of the mitochondrial carrier family with tissue-specific expression. *FEBS Lett.*, **408**, 39–42.

Bouillaud,F., Couplan,E., Pecqueur,C. and Ricquier,D. (2001) Homologues of the uncoupling protein from brown adipose tissue (UCP1): UCP2, UCP3, BMCP1 and UCP4. *Biochim. Biophys. Acta*, **1504**, 107–119.

Brand,M.D. (1995) Measurement of mitochondrial protonmotive force. In Brown,G.C. and Cooper,C.E. (eds), *Bioenergetics—A Practical Approach*. IRL Press, Oxford, UK, pp. 39–62.

Brand,M.D., Pamplona,R., Portero-Otin,M., Requena,J.R., Roebuck,S.J., Buckingham,J.A., Clapham,J.C. and Cadenas,S. (2002) Oxidative damage and phospholipid fatty acyl composition in skeletal muscle mitochondria from mice underexpressing or overexpressing uncoupling protein 3. *Biochem. J.*, **368**, 597–603.

Cadenas,S. *et al*. (2002) The basal proton conductance of skeletal muscle mitochondria from transgenic mice overexpressing or lacking uncoupling protein-3. *J. Biol. Chem.*, **277**, 2773–2778.

Chavez,E., Moreno-Sanchez,R., Torres-Marquez,M.E., Zazueta,C., Bravo,C., Rodriquez-Enriquez,S., Garcia,C., Rodriguez,J.S. and Martinez,F. (1996) Modulation of matrix Ca^{2+} content by the ADP/ATP carrier in brown adipose tissue mitochondria. Influence of membrane lipid composition. *J. Bioenerg. Biomembr.*, **28**, 69–76.

Chen,J.J. and Yu,B.P. (1994) Alterations in mitochondrial membrane fluidity by lipid peroxidation products. *Free Radic. Biol. Med.*, **17**, 411–418.

Chen,J.J., Bertrand,H. and Yu,B.P. (1995) Inhibition of adenine nucleotide translocator by lipid peroxidation products. *Free Radic. Biol. Med.*, **19**, 583–590.

Cohn,J.A., Tsai,L., Friguet,B. and Szweda,L.I. (1996) Chemical characterization of a protein-4-hydroxy-2-nonenal cross-link: immunochemical detection in mitochondria exposed to oxidative stress. *Arch. Biochem. Biophys*., **328**, 158–164.

Couplan,E., Del Mar Gonzalez-Barroso,M., Alves-Guerra,M.C., Ricquier,D., Goubern,M. and Bouillaud,F. (2002) No evidence for a basal, retinoic, or superoxide-induced uncoupling activity of the uncoupling protein 2 present in spleen or lung mitochondria. *J. Biol. Chem.*, **277**, 26268–26275.

Echtay,K.S., Winkler,E., Frischmuth,K. and Klingenberg,M. (2001) Uncoupling proteins 2 and 3 are highly active H^+ transporters and highly nucleotide sensitive when activated by coenzyme Q (ubiquinone). *Proc. Natl Acad. Sci. USA*, **98**, 1416–1421.

Echtay,K.S. *et al*. (2002a) Superoxide activates mitochondrial uncoupling proteins. *Nature*, **415**, 96–99.

Echtay,K.S., Murphy,M.P., Smith,R.A., Talbot,D.A. and Brand,M.D. (2002b) Superoxide activates mitochondrial uncoupling protein 2 from the matrix side. Studies using targeted antioxidants. *J. Biol. Chem.*, **277**, 47129–47135.

Esterbauer,H., Schaur,R.J. and Zollner,H. (1991) Chemistry and biochemistry of 4-hydroxynonenal, malonaldehyde and related aldehydes. *Free Radic. Biol. Med.*, **11**, 81–128.

Halliwell,B. and Gutteridge,J.M.C. (1999) *Free Radicals in Biology and Medicine*, 3rd edn. Oxford University Press, New York, NY.

Harper,J.A., Dickinson,K. and Brand,M.D. (2001) Mitochondrial uncoupling as a target for drug development for the treatment of obesity. *Obesity Rev.*, **2**, 255–265.

Humphries,K.M. and Szweda,L.I. (1998) Selective inactivation of alpha-ketoglutarate dehydrogenase and pyruvate dehydrogenase: reaction of lipoic acid with 4-hydroxy-2-nonenal. *Biochemistry*, **37**, 15835–15841.

Humphries,K.M., Yoo,Y. and Szweda,L.I. (1998) Inhibition of NADH-linked mitochondrial respiration by 4-hydroxy-2-nonenal. *Biochemistry*, **37**, 552–557.

Jekabsons,M.B., Echtay,K.S. and Brand,M.D. (2002) Nucleotide binding to human uncoupling protein-2 refolded from bacterial inclusion bodies. *Biochem. J.*, **366**, 565–571.

Kirichenko,A., Li,L., Morandi,M.T. and Holian,A. (1996) 4-hydroxy-2-nonenal-protein adducts and apoptosis in murine lung cells after acute ozone exposure. *Toxicol. Appl. Pharmacol.*, **141**, 416–424.

Klingenberg,M. (1975) The ADP–ATP carrier in mitochondrial membranes. *Enzymes Biol. Membr.*, **4**, 511–553.

Kristal,B.S., Park,B.K. and Yu,B.P. (1996) 4-Hydroxyhexenal is a potent inducer of the mitochondrial permeability transition. *J. Biol. Chem.* **271**, 6033–6038.

Musatov,A., Carroll,C.A., Liu,Y.C., Henderson,G.I., Weintraub,S.T. and Robinson,N.C. (2002) Identification of bovine heart cytochrome *c* oxidase subunits modified by the lipid peroxidation product 4-hydroxy-2-nonenal. *Biochemistry*, **41**, 8212–8220.

Nadkarni,D.V. and Sayre,L.M. (1995) Structural definition of early lysine and histidine adduction chemistry of 4-hydroxynonenal. *Chem. Res. Toxicol.*, **8**, 284–291.

Nohl,N. and Kramer,R. (1980) Molecular basis of age-dependent changes in the activity of adenine nucleotide translocase. *Mech. Ageing Dev.*, **14**, 137–144.

Papa,S. and Skulachev,V.P. (1997) Reactive oxygen species, mitochondria, apoptosis and aging. *Mol. Cell Biochem.*, **174**, 305–319.

Pecqueur,C., Alves-Guerra,M.C., Gelly,C., Levi-Meyrueis,C., Couplan,E., Collins,S., Ricquier,D., Bouillaud,F. and Miroux,B. (2001) Uncoupling protein 2, *in vivo* distribution, induction upon oxidative stress and evidence for translational regulation. *J. Biol. Chem.*, **276**, 8705–8712.

Portero-Otín,M., Pamplona,R., Ruiz,M.C., Cabiscol,E., Prat,J. and Bellmunt,M. (1999) Diabetes induces an impairment in the proteolytic activity against oxidized proteins and a heterogeneous effect in nonenzymatic protein modifications in the cytosol of rat liver and kidney. *Diabetes*, **48**, 2215–2220.

Rial,E., Gonzalez-Barroso,M., Fleury,C., Iturrizaga,S., Sanchis,D., Jimenez-Jimenez,J., Ricquier,D., Goubern,M. and Bouillaud,F. (1999) Retinoids activate proton transport by the uncoupling proteins UCP1 and UCP2. *EMBO J.*, **18**, 5827–5833.

Ricquier,D. and Bouillaud,F. (2000) The uncoupling protein homologues: UCP1, UCP2, UCP3, stUCP and atUCP. *Biochem. J.*, **345**, 161–179.

St-Pierre,J., Buckingham,J.A. Roebuck,S.J. and Brand,M.D. (2002) Topology of superoxide production from different sites in the mitochondrial electron transport chain. *J. Biol. Chem.*, **277**, 44784–44790.

Stuart,J.A., Harper,J.A., Brindle,K.M., Jekabsons,M.B. and Brand,M.D. (2001) A mitochondrial uncoupling artifact can be caused by expression of uncoupling protein 1 in yeast. *Biochem. J.*, **356**, 779–789.

Uchida,K. and Stadtman,E.R. (1992) Selective cleavage of thioether linkage in proteins modified with 4-hydroxynonenal. *Proc. Natl Acad. Sci. USA*, **89**, 5611–5615.

Ullrich,O., Henke,W., Grune,T. and Siems,W.G. (1996) The effect of the lipid peroxidation product 4-hydroxynonenal and of its metabolite 4-hydroxynonenoic acid on respiration of rat kidney cortex mitochondria. *Free Radic. Res.*, **24**, 421–427.

Vidal-Puig,A.J. *et al*. (2000) Energy metabolism in uncoupling protein 3 gene knockout mice. *J. Biol. Chem.*, **275**, 16258–16266.

Yan,L.J. and Sohal,R.S. (1998) Mitochondrial adenine nucleotide translocase is modified oxidatively during aging. *Proc. Natl Acad. Sci. USA*, **95**, 12896–12901.

Zhang,C.Y. *et al*. (2001) Uncoupling protein-2 negatively regulates insulin secretion and is a major link between obesity, beta cell dysfunction and type 2 diabetes. *Cell*, **105**, 745–755.

Zhang,Y.Q., Roote,J., Brogna,S., Davis,A.W., Barbash,D.A., Nash,D. and Ashburner,M. (1999) Stress sensitive B encodes an adenine nucleotide translocase in *Drosophila melanogaster*. *Genetics*, **153**, 891–903.

Received April 9, 2003; revised June 30, 2003; accepted July 1, 2003